

On the Radii of Brown Dwarfs Measured with *AKARI* Near-Infrared Spectroscopy

S. Sorahana^{1,2}, I. Yamamura² and H. Murakami²

¹Department of Astronomy, Graduate School of Science, The University of Tokyo,
Bunkyo-ku,

Tokyo 113-0033, Japan; sorahana@ir.isas.jaxa.jp

²Department of Space Astronomy and Astrophysics, Institute of Space and Astronautical
Science (ISAS),

Japan Aerospace Exploration Agency (JAXA), Sagami-hara, Kanagawa 252-5210, Japan

Received _____; accepted _____

Submitted to ApJ, 2012 October 14.

ABSTRACT

We derive the radii of 16 brown dwarfs observed by *AKARI* using their parallaxes and the ratios of observed to model fluxes. We find that the brown dwarf radius ranges between 0.64–1.13 R_J with an average radius of 0.83 R_J . We find a trend in the relation between radii and T_{eff} ; the radius is at a minimum at $T_{\text{eff}} \sim 1600$ K, which corresponds to the spectral types of mid- to late-L. The result is interpreted by a combination of radius–mass and radius–age relations that are theoretically expected for brown dwarfs older than 10^8 yr.

Subject headings: brown dwarfs – stars: low-mass – stars: radius

1. Introduction

Brown dwarfs are generally defined as the objects that are too light to maintain hydrogen fusion in their cores. For the solar metallicity, the upper limit of the brown dwarf mass, i.e., the hydrogen-burning main sequence edge mass, is $0.08 M_{\odot}$ (Kumar 1963; Hayashi & Nakano 1963). The lower edge of mass range of brown dwarfs overlaps with mass of planets. They are distinguished by their formation process instead of mass. Brown dwarfs are born in the interstellar medium through processes similar to that form stars. Objects that are born in protoplanetary disks should be referred to as planets.

The radii of brown dwarfs and planets in a context of their evolution are interesting subject. Radius of an exoplanet can be derived from photometric transit observations. On the other hand, it is difficult to determine a radius of a brown dwarf observationally, and that has not been discussed so far except for the objects in binary system. According to the theoretical study by Burrows et al. (2001) some brown dwarfs are actually smaller than Jupiter. The radii of brown dwarfs older than 10^9 yrs remain roughly constant at $0.7\text{--}1.1 R_J$ (R_J : Jupiter’s radius) for a broad mass range from 0.3 to $70 M_J$. Interestingly, more massive dwarfs have smaller radii. This fact is a consequence of the competition between two equations of state; Coulomb and electron degeneracy effects. Since the objects held by Coulomb effect would only set a fixed density, the relation of radius and mass follows $r \propto M^{1/3}$. On the other hand, electron degeneracy results in $r \propto M^{-1/3}$. Competition between two effects leads to the roughly constant radius–mass relation at $\geq 10^9$ yrs. Burgasser (2001) evaluated the expected radius of an observed brown dwarf by performing a Monte Carlo simulation adopting the evolutionary models by Burrows et al. (1997) with assumption of a constant birth rate and mass function $\frac{dN}{dM} \propto M^{-1}$. He found that the most likely radius is $0.9 \pm 0.1 R_J$.

Effective temperature (T_{eff}) of a brown dwarf has often been estimated empirically

by assuming its radius. Vrba et al. (2004) used a constant radius of $r = 0.9 R_J$ following Burgasser (2001) to estimate the empirical T_{eff} of 40 L and T dwarfs. They estimated T_{eff} from the equation $L = 4\pi R^2 \sigma T_{\text{eff}}^4$ (Drilling & Landolt 2000), where luminosity is derived from K -band flux by bolometric corrections. They reported that their derived T_{eff} for the early-L dwarfs, about 2400–2500 K, are warmer by about 200–300 K than some earlier estimates by fitting the spectral energy distributions with the synthetic spectra (e.g., Leggett et al. 2001). They argued that it is caused by different photometry database and slightly different assumptions of brown dwarf radii.

Yamamura et al. (2010) analyzed 2.5–5.0 μm spectra of six brown dwarfs taken by the Japanese infrared astronomical satellite *AKARI* (Murakami et al. 2007). They found that T_{eff} derived by the Unified Cloudy Model (UCM; Tsuji 2002, 2005) fitting to the observed spectra are lower by typically 200 K from the empirical T_{eff} estimated by Vrba et al. (2004). They also reported that the radii derived from the *AKARI* observations have an average value of $0.81 R_J$, and distribute in a wider range between 0.68 – $1.18 R_J$ than that expected from Burrows et al. (2001). They argued that the radii of brown dwarfs should not be represented by a single mean value.

In this paper, we discuss the radii of an extended sample of brown dwarfs determined by the *AKARI* observations in detail. First, we introduce our objects in Section 2, and outline our fitting procedure briefly in Section 3¹. We describe a method of deriving radius of brown dwarfs and uncertainty of the radius in Section 4. We present the resulted radii of 16 observed brown dwarfs in Section 5, and discuss the relation between radius and T_{eff} and their evolutionary status in Section 6.

¹The details of data reduction, calibration and fitting process are described in Sorahana & Yamamura (2012).

2. The *AKARI* Sample

Twenty seven brown dwarfs including 16 L dwarfs and 11 T dwarfs were observed by *AKARI*. Our targets selected by their expected fluxes to be bright enough for Infrared Camera (IRC) onboard the *AKARI* to provide high-quality spectra within the reasonable amount of exposures and their spectral types to sample various types from L to T. We obtained good quality spectra of 16 brown dwarfs included 11 L and 5 T dwarfs (Table 1).

These 16 objects are nearby and bright, thus they are generally well studied. There are three binaries in this sample, GJ 1001B, 2MASS J1523+3014 and Gl 570D. 2MASS J1523+3014 is as known as Gl 584C and is a companion of Gl 584AB, which is a G dwarf double. 2MASS J1523+3014 is widely (194") separated from Gl 584AB (Kirkpatrick et al. 2000). Gl 570D is a companion of Gl 570ABC triple system, and is also located 258" from Gl 570ABC (Burgasser et al. 2000). In our observation, the target source was placed in the 1×1 arcmin² aperture of the *AKARI*/IRC instrument. Therefore, 2MASS J1523+3014 and Gl 570D were observed without confusion from their primary stars. On the other hand, GJ 1001B is located only 18.2" from the primary M dwarf GJ 1001A (Goldman et al. 1999) and the spectrum of GJ 1001B was contaminated by a shoulder of an intense signal from GJ 1001A. We evaluated and subtracted the signal from GJ 1001A at the position of GJ 1001B (see Sorahana & Yamamura 2012 for detail). Golimowski et al. (2004) found that GJ 1001B also has a companion GJ 1001C separated by 0.087". The two dwarfs are of the similar spectral types. To derive the radius of GJ 1001B (or C; hereafter GJ 1001B), we assume that the luminosity of each dwarf is a half of the observed one. All other objects in our sample are believed to be single sources.

Table 1. Sixteen Brown Dwarfs observed by *AKARI*

Object Name	Sp. Type	$T_{\text{eff}}[\text{K}]$	Parallax(error)[mas]	Binary	References
2MASS J14392836+1929149	L1	2100	69.6(0.5)	No	1, a
2MASS J00361617+1821104	L4	2000	114.2(0.8)	No	2, a
2MASS J22244381–0158521	L4.5	1800	85.0(1.5)	No	1, b
GJ 1001B	L5	1800	76.9(4.0)	Yes	1, c
SDSS J144600.60+002452.0	L5	1800	45.5(3.3)	No	2, b
SDSS J053951.99–005902.0	L5	1800	76.1(2.2)	No	2, b
2MASS J15074769–1627386	L5	1800	136.4(0.6)	No	1, a
2MASS J08251968+2115521	L6	1500	95.6(1.8)	No	2, b
2MASS J16322911+1904407	L7.5	1500	63.6(3.3)	No	2, b
2MASS J15232263+3014562	L8	1600	57.3(3.3)	Yes	2, b
SDSS J083008.12+482847.4	L9	1600	76.4(3.4)	No	2, b
SDSS J125453.90–012247.4	T2	1400	75.7(2.9)	No	2, b
SIMP J013656.5+093347.3	T2.5	1400	6.4(0.3)	No	3, d
2MASS J05591914–1404488	T4.5	1200	95.5(1.4)	No	2, b
Gliese 570D	T8	700	169.3(1.7)	Yes	2, a
2MASS J04151954–0935066	T8	700	174.3(2.8)	No	3, b

Note. — Reference of spectral type (1) Kirkpatrick et al. (2000), (2) Geballe et al. (2002), (3) Burgasser et al. (2006).

The parallaxes are referred from (a) Dahn et al. (2002), (b) Vrba et al. (2004), (c) Henry et al. (2006), and (d) Artigau et al. (2006).

The number given for SIMP J0136+0933 is a photometric distance [pc] estimated by comparing the spectral energy distribution with known brown dwarfs of similar spectral types.

3. Best Fit Model Derived from *AKARI* Near-Infrared Spectra

We derived physical parameters of brown dwarfs, namely effective temperature T_{eff} , surface gravity $\log g$ and critical temperature T_{cr} by model fitting with UCM. T_{cr} is a temperature below which the dust disappears by sedimentation or other unknown mechanism, and given as an additional parameter in UCM, i.e., the dust would exist in the layer with $T_{\text{cr}} < T < T_{\text{cond}}$. T_{cr} is not predictable by any physical theory at present and is required to be determined from observations empirically. We mainly use *AKARI* spectra in the range of 2.5–4.15 μm (not to 5.0 μm because the current model does not explain the observed spectra beyond 4.15 μm . See Yamamura et al. 2010). We follow Cushing et al. (2008) and evaluate the goodness of the model fitting by the statistic G_k defined as

$$G_k = \frac{1}{n - m} \sum_{i=1}^n \omega_i \left(\frac{f_i - C_k F_{k,i}}{\sigma_i} \right)^2, \quad (1)$$

where n is the number of data points; m is degree of freedom (this case $m = 3$); ω_i is the weight for the i -th wavelength points (we give the equal weight as $\omega_i = 1$ for all data points because of no bias within each observed spectrum); f_i and $F_{k,i}$ are the flux densities of the observed data and k -th model, respectively; σ_i are the errors in the observed flux densities and C_k is the scaling factor given by

$$C_k = \frac{\sum \omega_i f_i F_{k,i} / \sigma_i^2}{\sum \omega_i F_{k,i}^2 / \sigma_i^2}. \quad (2)$$

G_k is equivalent to reduced χ^2 , since we adopt $\omega_i = 1$ in our analysis. It is difficult to determine a unique best-fit model for each object because of relatively large error associated with the *AKARI* spectra. Thus we also use the shorter wavelength spectra (IRTF/Spex and UKIRT/CGS4 data) to complete our analysis. Details of fitting evaluation are described in Sorahana & Yamamura (2012). We show an example of model fitting in Figure 1. This object, 2MASS J2224–0158 is a relatively warm object of the spectral type L4.5.

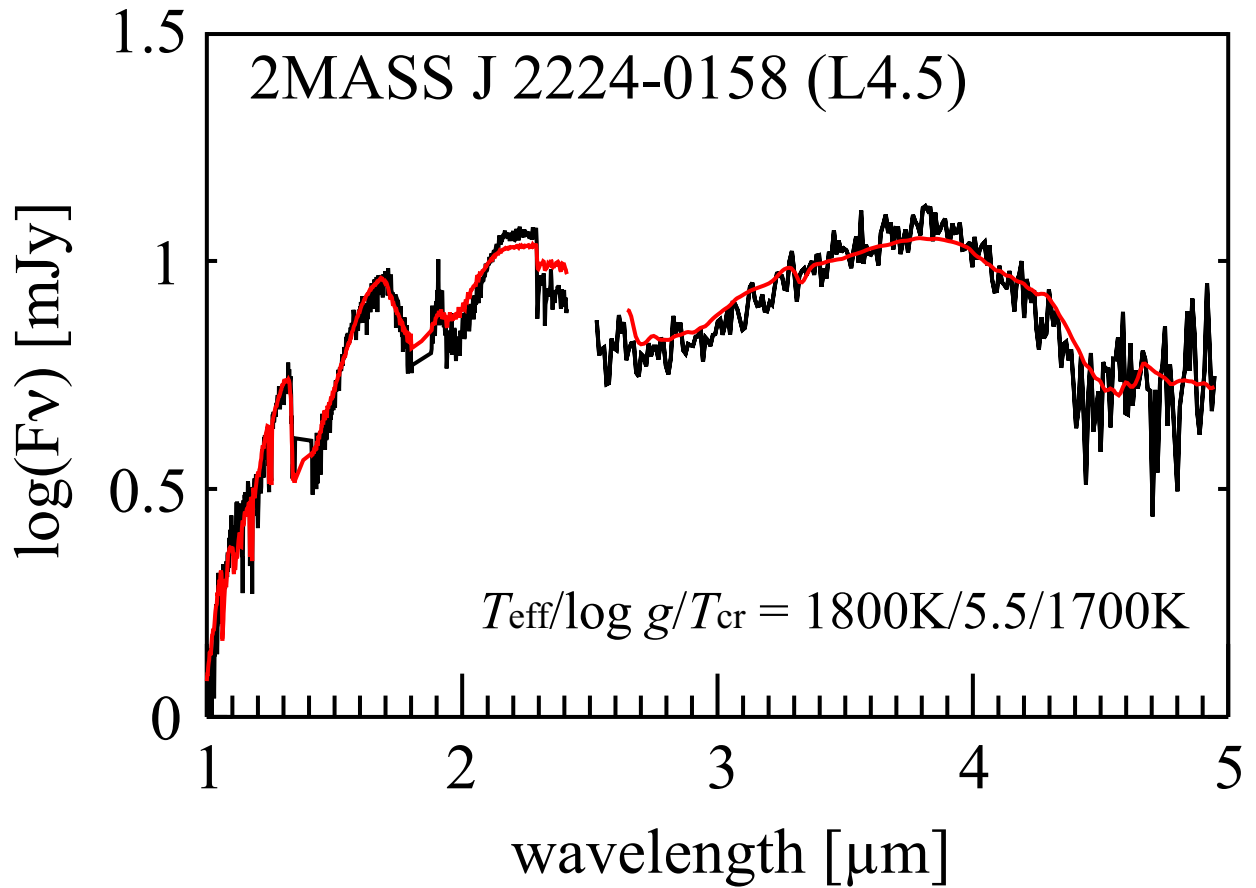


Fig. 1.— The observed and the best fit model spectra for 2MASS J2224–0158 (L4.5). The black line is the observed data and the red line is the best-fit model spectra. The spectrum between 2.5 and 5.0 μm is taken by *AKARI* and that between 1.0 and 2.5 μm is taken by IRTF/SpeX. The parameters of the best fit model are given in the legend of the figure.

4. Radius of Brown Dwarfs

4.1. Derivation of the Radius

The ratio of model flux F_ν [erg/s/cm²/Hz], which is for a unit radius at a unit distance, to observed flux f_ν [mJy] is written as

$$\log(F_\nu/f_\nu) = -2 \log(r/D) - 26.497, \quad (3)$$

where r is the radius and D is the distance. D of each object has been calculated from its parallax given in the 4th-column of Table 1, except for SIMP J0136+0933 for which the value is a spectrophotometric estimate. Distance of SIMP J0136+0933 is estimated by comparing the flux with known brown dwarfs of similar spectral types (Artigau et al. 2006). The model flux F_ν is from the UCM best fit model spectra given by Sorahana & Yamamura (2012). Equation (3) is written with C of the best fit model as,

$$\frac{C}{10^{26.497}} = \left(\frac{r}{D}\right)^2. \quad (4)$$

4.2. Uncertainty of the Radius

The radius in this analysis relies on the distance D and the flux scaling factor C defined in Equation (2). The uncertainty of D is estimated from the parallax error shown in Table 1. The maximum error of D is $\sim 7\%$. Some brown dwarfs have multiple parallax measurements and the results are consistent to each other within the error. The uncertainty of C depends on the absolute flux calibration of *AKARI* spectra and the goodness of the model fitting. The former is evaluated to be about 10% (Ohyama et al. 2007), and was also validated with L' photometry data in Sorahana & Yamamura (2012). The latter error is different for each object. Model spectra do not yet perfectly reproduce the observed spectra because of for example an incomplete CH₄ line list and unknown properties of dust in the

photosphere not yet incorporated into the model (Yamamura et al. 2010). Hence it is hard to find a unique best-fit model. Sorahana & Yamamura (2012) discussed the uncertainty of the best-fit model parameters. The uncertainty should be no better than a half of the grid spacing (100 K for T_{eff} and T_{cr} and 0.5 dex for $\log g$). To estimate the uncertainty we change each of T_{eff} , $\log g$, and T_{cr} by one grid from the best-fit value, and search for the “restricted best” model by changing other two parameters following the same manner through fitting evaluation. If we do not find any models satisfying $G_{\text{min}} \leq G_k < G_{\text{min}} + 1$ (here, G_{min} is taken from all parameter space in model fitting with *AKARI* data only), then the uncertainty of the parameter should be smaller than the grid spacing. In order to estimate the uncertainty of C , we evaluate the ratio of C' for the “restricted best” model to C for the best model. The maximum deviation of C'/C from 1.0 is $\sim 30\%$. The resulted overall error of derived radius is listed in Table 2. Uncertainty of radius ranges between 5 % and 16 %. The uncertainty is the largest for 2MASS J0559–1404 because of the large C error.

5. Results

The result is listed in Table 2. The average radius of 16 brown dwarf samples is $0.83 R_J$ with a standard deviation of $0.14 R_J$. The average is slightly smaller than the value given by Burgasser (2001), but is consistent within the uncertainty. The derived radii ranges from 0.64 to $1.13 R_J$. Figure 2 shows the relation between T_{eff} and radii at different masses from $11 M_J$ to $0.085 M_{\odot}$ predicted by evolutionary model of Burrows et al. (2001), and our results are over-plotted with uncertainties. Our results are consistent with theoretical predictions for early-L and T dwarfs.

From this figure we can discuss mass and age of the objects. Both masses and ages of 2MASS J0036+1821 and 2MASS J2224–0158 are similar to each other, though their T_{eff}

are different. Ages of 2MASS J1439+1929 and 2MASS J0559–1404 are close (relatively younger than other objects) to each other, but their masses are quite different. Likewise, SDSS J1254–0122 and 2MASS J0415–0935 are in similar ages, but with different masses. On the other hand, masses of 2MASS J0559–1404 and Gl 570D are close to each other, but ages are not; 2MASS J0559–1404 is younger than that of Gl 570D. The age of Gl 570D is estimated by Kirkpatrick et al. (2001) as 2–10 Gyr, and is consistent with our result within its uncertainty.

Our sample includes objects with very small radii. Radii of GJ 1001B, 2MASS J1523+3014, SDSS J0830+4828, SDSS 1446+0024 and 2MASS J1507–1624 are 0.64, 0.65, 0.66, 0.74 and 0.79, respectively. They are out of range of the theoretical predictions. Interestingly those small radii objects are all around $T_{\text{eff}} \sim 1600$ K, i.e., the radii of our brown dwarfs hold minimum at mid- to late-L, though we apply some assumptions for GJ 1001B through the data analysis.

6. Discussion

We find that the radii of mid- to late-L objects with $T_{\text{eff}} \sim 1600$ K are smaller than those of theoretical predictions in absolute scale, and those of early-L and T dwarfs in relative scale. In this section, we discuss these results.

6.1. Validity of Our Result

First, we verify the absolute values of our resultant radii. A fair comparison with the theoretical prediction needs a mass and an age of each brown dwarf. However, it is difficult to measure the accurate mass and age of each object observationally unless the objects are members of a cluster or a binary. If the object is unresolved binary for *AKARI*, their radius

should be even smaller. Mass can be evaluated from the surface gravity. However, the uncertainty of mass of each object is very large because of the large uncertainty in surface gravity derived by the model fitting (Sorahana & Yamamura 2012).

We can justify our result in another way. If we assume that the radius of 2MASS J1523–3014 is the mean value $0.83 R_J$, the flux levels should be 1.6–1.7 times higher. This is unreasonably larger than the error in the flux calibration, and we regard that the radii of mid- to late-L dwarfs should be as small as $0.7 R_J$. It is noted that the spectra of mid- to late-L dwarfs are most affected by the dust in the atmosphere. The incompleteness in the atmosphere model could draw a systematic error in the flux level. However, we do not see any particular jumps in the flux levels of the models along the changes of the model parameters, indicating that 60–70 % changes in the flux level should not be accounted by the model.

Recently, Burrows et al. (2011) discuss metallicity dependence of brown dwarf radii. In fact we argue that our *AKARI* sample may have metallicity variation (Tsuji et al. 2011; Sorahana et al. in prep.). However, the expected change of radius is as much as several per cent still much smaller than the discrepancy we found here.

We conclude that the radii derived from our observed data are regarded to be real and admit there exists a serious deviation between observation and evolutionary model.

6.2. Radius Inversion

Our *AKARI* sample is selected by their spectral types to sample various types from L to T, and may be biased to some extent. They locate very close to our sun (5–25 pc), thus we expect that they are as old as the sun ($\sim 10^{9.7}$ yrs). Ages of three binaries in our sample, GJ 1001B, 2MASS J1523+3014 and Gl 570D, are determined by Kirkpatrick et al.

(2001) to be 1 Gyr, 1-2.5 Gyr and 2-10 Gyr, respectively. The ages of our objects can also be evaluated from Figure 2, as we discussed in this section. Those of mid- to late-L dwarfs are out of the theoretical evolutionary tracks but they are likely older than 10^8 yr. Our results indicate older ages for GJ 1001B and 2MASS J1523+3014. While theory allows a wide variety of mass for T dwarfs, all L dwarfs at near solar age are massive objects (See Figure 8 of Burrows et al. 2001). In other words, it is highly possible that L dwarfs of our sample are more massive than our T dwarfs. On the other hand, Figure 2 tells that early-L dwarfs in our sample (e.g., 2MASS J439+1929, 2MASS J0036+1821) are relatively younger and less massive than mid- to late-L objects.

Brown dwarfs shrink slowly as they evolve. As previously noted, the radii of brown dwarfs do not follow a monotonic function of mass, in particular after the age of $10^{7.5}$ yrs. According to Burrows et al. (2001), the radius of a less massive object is already small at its formation and change of radius during its lifetime is also small. On the other hand, the radius of a massive object is large when it is young, but become smaller than the lighter objects beyond $\sim 10^8$ yrs, because the electron degeneracy effect overcomes the coulomb effect. This inversion of radius takes place continuously in the mass range between 0.3 and $70 M_J$. The relation of radius and mass with age is shown in Figure 3. The data are provided from Adam Burrows (in priv. comm.). We see a depression on the curves for the dwarfs older than 10^8 yrs, which indicates the radius inversion by the degeneracy effect. A sharp bump at $\sim 0.015 M_\odot$ is due to a deuterium burning. The horizontal axes of Figure 2 and 3 are not simply equivalent, because effective temperature T_{eff} (spectral type) of a brown dwarf depends on both mass and age. According to the discussions above, the trend in our *AKARI* sample can be explained by a combination of both effects. Early types that the effective temperature ranges between 1500 and 2100 K tend to depend on their age as shown in Figure 2. We show this trend by overlaying a red arrow in Figure 3. On the other hand, late-types with T_{eff} lower than 1500 K is more mass dependent than age. The trend

is described by a blue arrow in Figure 3. Our result of the relation of radii against their T_{eff} implies that inversion of radius predicted by theory is actually taking place.

7. Conclusion

We derive the radii of 16 brown dwarfs observed by *AKARI* by comparing model flux and observed flux at given distances. The resulted radii ranges in 0.64–1.13 R_J . The average radius is 0.83 R_J with a standard deviation of 0.14 R_J . Our results are consistent with the theoretical radii calculated by Burrows et al. (2001) within the error for early-L and late-T dwarfs, however, a large discrepancy is found for some mid- and late-L dwarfs. We find that the radii of mid- to late-L dwarfs are smaller than theoretical prediction. We verify that our estimates of radius is reasonable, and conclude that there are deviation between observation and evolutionary model. We can not find any reason of this deviation and leave it to the future studies. We also find that the radii reach a minimum for the mid- to late-L dwarfs. Theory predicts that there is an inversion in the radius–mass relation in the brown dwarfs older than 10^8 yrs. Our results confirm that this theoretical prediction of radius inversion actually present.

We thank to the anonymous referee for critical reading of our article and constructive suggestions. This research is based on observations with *AKARI*, a JAXA project with the participation of ESA. We thank to Prof. Takashi Tsuji for his kind permission to access the UCM and helpful suggestions. Prof. Adam Burrows kindly provide us the numerical data and warm encouragement. We acknowledge JSPS (PI: S. Sorahana) and JSPS/KAKENHI(c) No. 22540260 (PI: I. Yamamura).

Table 2. The radius of *AKARI* objects

Object Name	Sp. Type	Radius(error) [R_J]	Number in Figure 2
2MASS J1439+1929	L1	1.01(0.05)	1
2MASS J0036+1821	L4	0.88(0.05)	2
2MASS J2224-0158	L4.5	0.87(0.05)	3
GJ 1001B	L5	0.64(0.05)	4
SDSS J1446+0024	L5	0.74(0.06)	5
SDSS J0539-0059	L5	0.82(0.05)	6
2MASS J1507-1627	L5	0.79(0.06)	7
2MASS J0825+2115	L6	0.76(0.09)	8
2MASS J1632+1904	L7.5	0.74(0.10)	9
2MASS J1523+3014	L8	0.65(0.09)	10
SDSS J0830+4828	L9	0.66(0.08)	11
SDSS J1254-0122	T2	0.84(0.05)	12
SIMP J0136+0933	T2.5	0.80(0.12)	13
2MASS J0559-1404	T4.5	1.13(0.18)	14
G1 570D	T8	1.04(0.05)	15
2MASS J0415-0935	T8	0.94(0.05)	16

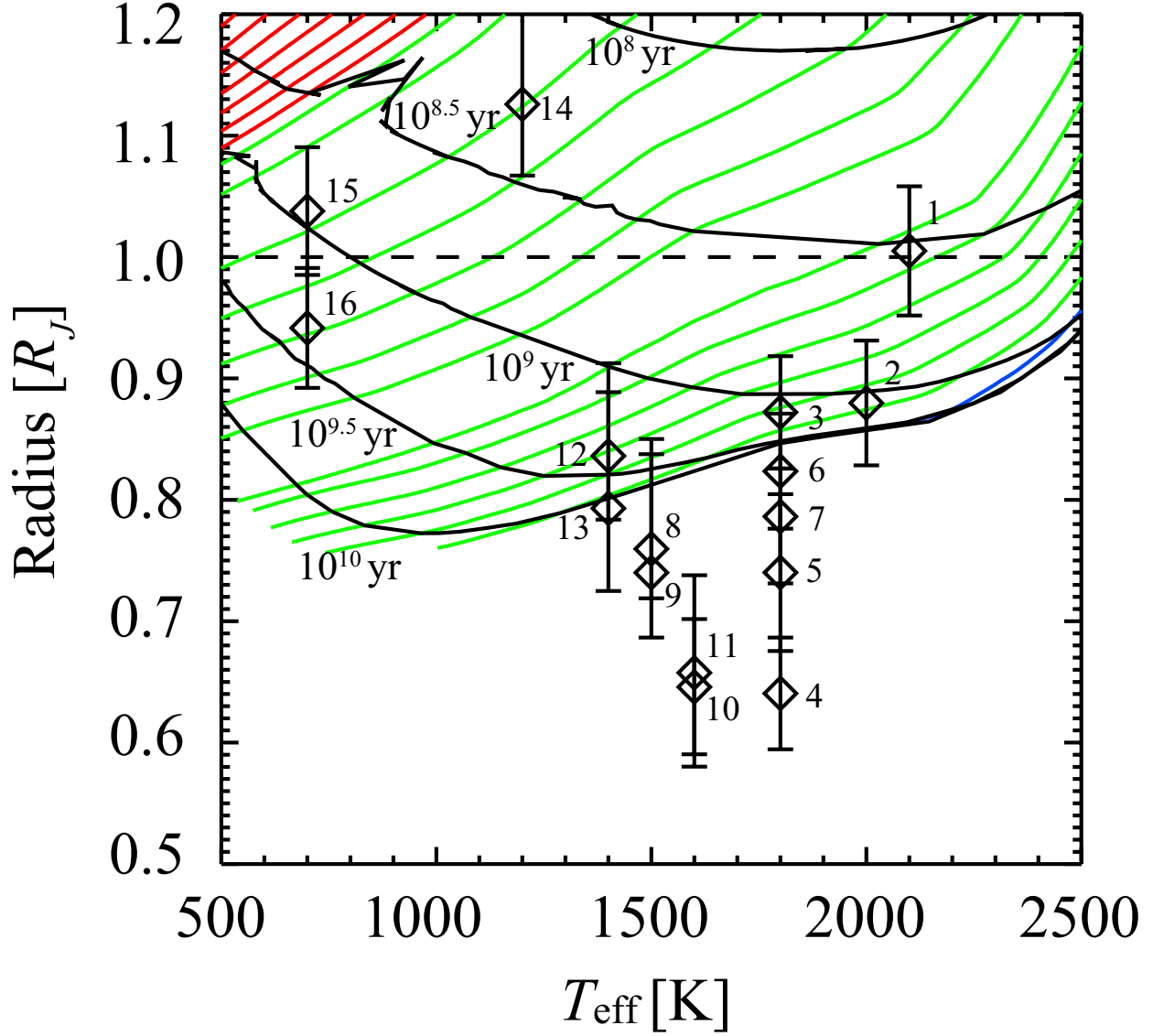


Fig. 2.— The radii of *AKARI* observed brown dwarfs are plotted on theoretical prediction of the relation between T_{eff} and radii at different masses from $11 M_J$ to $0.085 M_\odot$. Red are less massive objects with 11, 12, 13 and $15 M_J$, blue are massive objects 0.08 and $0.085 M_\odot$ and green are intermediate mass objects with 0.02 , 0.025 , 0.03 , 0.035 , 0.04 , 0.045 , 0.05 , 0.055 , 0.06 , 0.065 , 0.07 and $0.075 M_\odot$. The numerical data of evolutionary model are provided by Adam Burrows (in private communication). The numbers are object index in Table 2.

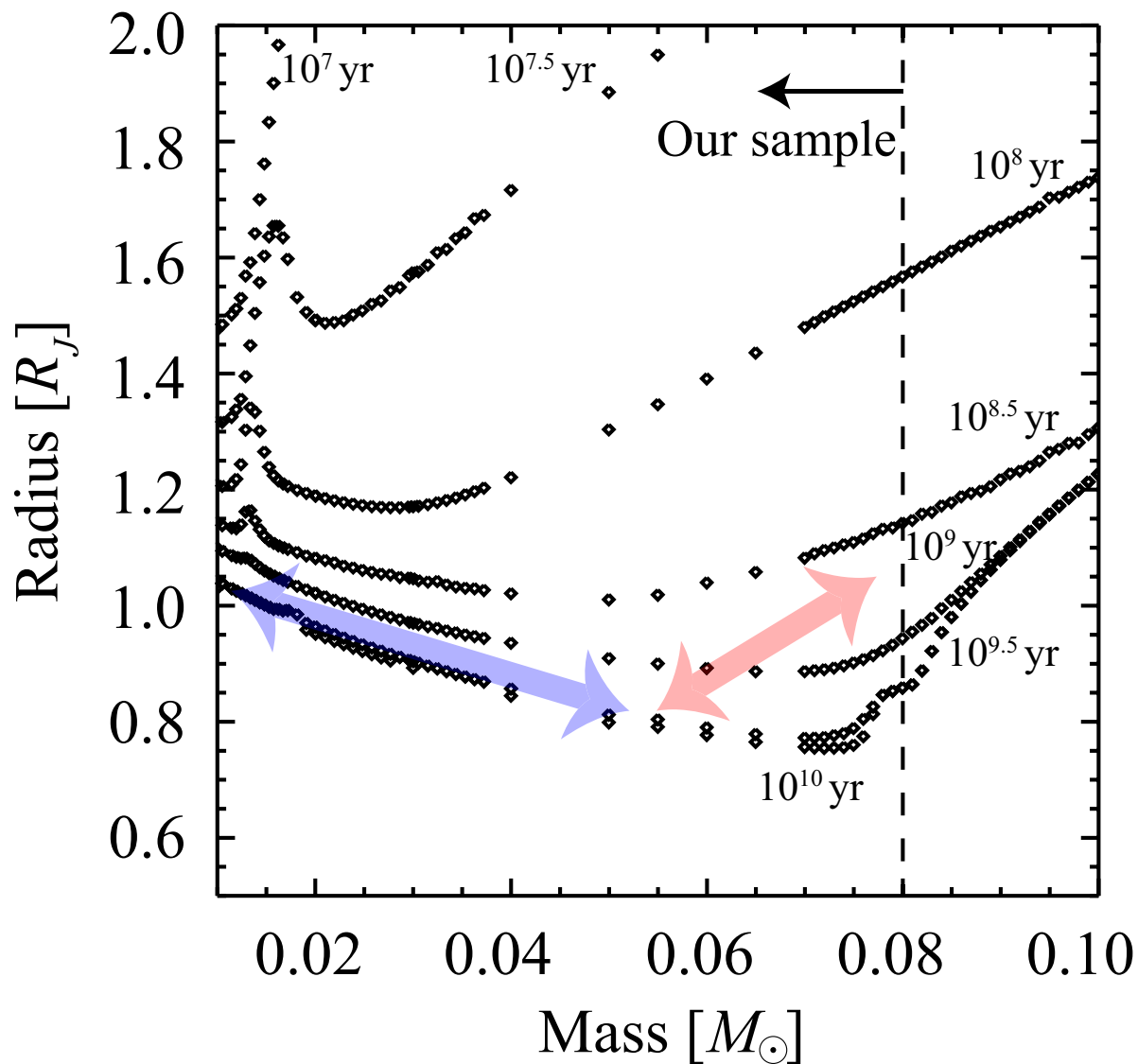


Fig. 3.— Theoretical prediction of the relation between radius and mass of brown dwarfs at different ages. The radii of relatively light and young objects are small and rather stable throughout their lifetimes. On the other hand, the radii of massive dwarfs $\geq 0.06 M_{\odot}$ are large when they are young, but ultimate radii are smaller than those of less massive objects. The radii of early-type objects in our sample tend to depend on their age (shown by red arrow), while those of late-type objects tend to depend more on their mass than their age (shown by blue arrow). The data are provided by Adam Burrows (in private communication).

REFERENCES

- Artigau, É., Doyon, R., Lafrenière, D., et al. 2006, *ApJ*, 651, L57
- Burgasser, A. J. 2001, PhD thesis, Department of Physics, California Institute of Technology
- Burgasser, A. J., Geballe, T. R., Leggett, S. K., Kirkpatrick, J. D., & Golimowski, D. A. 2006, *ApJ*, 637, 1067
- Burgasser, A. J., Kirkpatrick, J. D., Cutri, R. M., et al. 2000, *ApJ*, 531, L57
- Burrows, A., Heng, K., & Nampaisarn, T. 2011, *ApJ*, 736, 47
- Burrows, A., Hubbard, W. B., Lunine, J. I., & Liebert, J. 2001, *Reviews of Modern Physics*, 73, 719
- Burrows, A., Marley, M., Hubbard, W. B., et al. 1997, *ApJ*, 491, 856
- Cushing, M. C., Marley, M. S., Saumon, D., et al. 2008, *ApJ*, 678, 1372
- Dahn, C. C., Harris, H. C., Vrba, F. J., et al. 2002, *AJ*, 124, 1170
- Drilling, J. S., & Landolt, A. U. 2000, *Allen’s Astrophysical Quantities*, ed. A. N. Cox (New York: Springer), 381
- Geballe, T. R., Knapp, G. R., Leggett, S. K., et al. 2002, *ApJ*, 564, 466
- Goldman, B., Delfosse, X., Forveille, T., et al. 1999, *A&A*, 351, L5
- Golimowski, D. A., Henry, T. J., Krist, J. E., et al. 2004, *AJ*, 128, 1733
- Hayashi, C., & Nakano, T. 1963, *Progress of Theoretical Physics*, 30, 460
- Henry, T. J., Jao, W.-C., Subasavage, J. P., et al. 2006, *AJ*, 132, 2360
- Kirkpatrick, J. D., Dahn, C. C., Monet, D. G., et al. 2001, *AJ*, 121, 3235

- Kirkpatrick, J. D., Reid, I. N., Liebert, J., et al. 2000, *AJ*, 120, 447
- Kumar, S. S. 1963, *ApJ*, 137, 1121
- Leggett, S. K., Allard, F., Geballe, T. R., Hauschildt, P. H., & Schweitzer, A. 2001, *ApJ*, 548, 908
- Murakami, H., Baba, H., Barthel, P., et al. 2007, *PASJ*, 59, S369
- Ohyama, Y., Onaka, T., Matsuhara, H., et al. 2007, *PASJ*, 59, S411
- Sorahana, S., & Yamamura, I. 2012, *ApJ*, 760, 151
- Tsuji, T. 2002, *ApJ*, 575, 264
- . 2005, *ApJ*, 621, 1033
- Tsuji, T., Yamamura, I., & Sorahana, S. 2011, *ApJ*, 734, 73
- Vrba, F. J., Henden, A. A., Luginbuhl, C. B., et al. 2004, *AJ*, 127, 2948
- Yamamura, I., Tsuji, T., & Tanabé, T. 2010, *ApJ*, 722, 682